International Journal of Industrial Electronics, Control and Optimization © 2019 IECO
Vol. 2, No. 2, pp. 145-154, April (2019)

Microgrid frequency control using the virtual inertia and ANFIS-based Controller

Akbar Karimipouya[1], Shahram karimi [†2] and Hamdi Abdi[3]

[†,1,2,3] Department of Electrical Engineering, Razi university, Kermanshah, Iran

ABSTRACT

The main challenge in associate islanded Micro grid (MG) is the frequency stability due to the inherent low-inertia feature of distributed energy resources. That is why, energy storage devices, are utilized in MGs as the promising sources for grid short-term frequency regulation. Though energy storage devices, improve the dynamic operation of the load-frequency control (LFC) system, these devices increase system costs. Moreover, the modification or uncertainty of the system parameters will significantly degrade the performance of the conventional LFC system. This article proposes the execution of rotating-mass-based virtual inertia in Double-Fed Induction Generator (DFIG) to support the first frequency control associated an adaptive Neuro-Fuzzy inference System (ANFIS) controller, as secondary frequency control. The simulation conclusions illustrate that the suggested control scheme ameliorate the dynamic operation of the LFC system and also the studied islanded MG remains stable, despite severe load variation and parametric uncertainties.

Article Info

Keywords:
Microgrid, Frequency Control,
DFIG, Virtual Inertia, Fuzzy PID Controller, ANFIS.

Article History:
Received 2018-08-05
Accepted 2018-12-09

I. INTRODUCTION

In recent decades, the use of renewable energy has enhanced, the main cause of which is environmental pollution and economic aspects [1]. Wind energy has become one in all the most necessary renewable energies and the largest view in terms of new technologies and economical. Due to the variable speed of wind, for maximum efficiency at different speeds, the turbine with variable speed is required [2,3]. Therefore, the wind turbine equipped with Double-Fed Induction Generators (DFIGs) are widely utilized in Wind Energy Conversion System (WECS) [4]. There is generally no inertia response between the DFIG rotor speed and the frequency of the system. There is additionally no primary frequency regulation and only the maximum power point tracking (MPPT) method is used in DFIG power control system [5]. Therefore, with high wind power penetration, inevitably there are major challenges in frequency regulation. In addition, the main challenge in an islanded Micro grid (MG) is the frequency stability due to the inherent low-inertia feature of Distributed Energy Resources (DERs). That is why, energy storage equipment, because of their rapid response time and ability to charge and discharge efficiently, are used in MGs as the promising sources for grid short-term frequency regulation [6]. Although energy storage instruments, like batteries, flywheels, and super-capacitors, improve the dynamic operation of the Load-Frequency control (LFC) system, these devices, along with their respective inverter, increase system costs.

Wind turbines participation in frequency adjustment is the idea to make better the dynamic frequency respond characteristics of power systems. In [7-15], by implementing virtual inertia in DFIG control system, the dynamic behavior of the MG is improved. In [7, 8], the primary frequency control strategy, virtual inertia and blade angle control are used in DFIG to reduce the frequency variation. In [9, 10], the super-capacitor, as the source of inertia, has been used. In [11], using double-layer capacitor energy storage, dynamic stability is improved. These methods also, due to the use of additional equipment, is costly. In [12-15], the inertia of the wind turbine rotating mass is used to implement virtual inertia in DFIG control system. Although implementation of

[†] **Corresponding Author**: shahramkarimi@razi.ac.ir
[*] Electrical Engineering Department, Razi University, Kermanshah, Iran

virtual inertia with rotating masses does not require additional equipment and costs, its implementation is subject to some limitations. In this method, the virtual inertia appertain to the wind speed, and therefore, its value is completely variable and stochastic. Another limitation to the use of rotating-mass-based virtual inertia is a thermal constraint. At high wind speeds, frequency deviation leads to the additional power generation, due to the virtual inertia control loop, and consequently, the temperature of the DFIG rises, which may be more than allowed [13]. Moreover, in this paper, it is shown that the change or uncertainty of the system parameters, such as droop factor, can considerably degrade the performance of the LFC system.

Contrariwise, in the conventional LFC systems, the PI or PID controllers are usually used as secondary frequency control. Although these controllers have such advantages as simplicity and easy implementation, they are mostly used for systems with simple and constant configuration. Therefore, because the structure and configuration of micro grids are constantly changing and there are many uncertainties, conventional controllers with constant parameters cannot be used. [15]. Also, Most of the linearization methods used to control the frequency increase the system's order, which makes the micro grid more complicated [16].

Fuzzy logic and neural controllers also have been developed in many control applications to intricate models [17]. The fuzzy is based on the rules "if and then", which we get these rules from the system description. Since we do not have much information about the behavior of most systems, conclusion from these types of systems is difficult and neural controllers need a lot of time for training. Combined methods are among the methods developed to control complex systems in recent years. One of these combined algorithms is Adaptive Neuro-Fuzzy Inference System (ANFIS). An ANFIS benefits from both fuzzy and neural control systems. In this paper, instead of the conventional PID controller, an ANFIS-based controller is proposed to use as secondary frequency control while the rotating-mass-based virtual inertia is implemented to support the primary frequency control.

So far, several intelligent controllers have been explored as complementary frequency control of micro grids. In [6], frequency control has been improved using the fuzzy-PSO method with the amount of electric power generated by wind turbines. In [18], frequency control has been improved using the HPSO algorithm decentralized. In [19] using fuzzy logic, control for the micro grid frequency is done with high penetration of wind turbines. In [20], frequency control is performed using an on-line method that detects frequency variations using PSO and fuzzy algorithms. But until now, research on the use of ANFIS-based controller as complementary frequency control of the micro grid has not been reported when virtual inertia is involved in the LFC system.

The rest of this study is segmented as follows: The second part describes the model of the micro grid studied. In Section 3, the implementation of rotating-mass-based virtual inertia in DFIG are explained. Fuzzy PID and ANFIS-based controllers' design are addressed in part 4. Results and simulations of different controllers and their comparison are presented in part 5. Eventually, the general conclusion is summarized in part 6.

II. THE STUDIED MG STRUCTURE

Figure 1 shows an islanded micro grid containing various DGs. This system includes wind turbine, solar cell, diesel generator, fuel cell, battery and flywheel storage devices. The parameters of the studied MG are also presented in Table 1.

In the studied MG, as shown in Fig. 1, diesel generator consists of the primary and complementary frequency control loop Also, a complementary frequency control loop; control the fuel cell output power. Droop control is used for the primary frequency control and the storage devices are used for supporting the primary frequency control. Different controllers are designed for the secondary frequency control loops. These controllers are the classical PID controller, PID fuzzy and proposed ANFIS-based controller.

TABLE I. MICRO GRID PARAMETERS

Parameter	Value	Parameter	Value
D(Pu/Hz)	0.015	$T_g(s)$	0.08
2H(Pu s)	0.1667	$T_t(s)$	0.4
$T_{Fess}(s)$	0.1	$T_{I/c}(s)$	0.004
$T_{Bess}(s)$	0.1	$T_{in}(s)$	0.04
$T_{FC}(s)$	0.26	R(Hz/Pu)	3

TABLE II . NOMINAL POWER OF DG UNITS AND LOAD

Rated Power (kW)		Load (kW)
WTG	100	430
PV panel	30	
FC	70	
DEG	160	
FESS	45	
BESS	45	

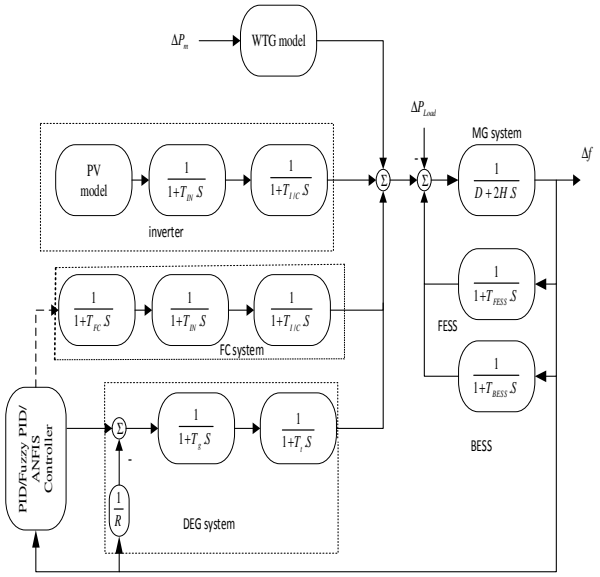


Fig.1. schematic block diagram of the studied islanded MG.

III. IMPLEMENTING VIRTUAL INERTIA

In a DFIG, stator directly and rotor via two converters connected to the power system. It produces the highest wind power using a converter that is located on the rotor's side and it adjusts the stator voltage. DC voltage can be adjusted using the network side converter. Wind turbines such as synchronous generators have high inertia, which this energy is stored as kinetic in its axis. However, this energy cannot participate in frequency adjusting due to the decoupled mechanical and electrical power controllers.

The maximum power that can be obtained from a wind turbine, Pm, opt can be expressed

$$P_{m,opt}=K_{opt}\omega_m^3 \tag{1}$$

Where ωm is DFIG rotational speed and Kopt is fixed when the angle of the turbine blade is constant.

The input mechanical and the output electrical powers (Pm, Pe) are related to each other as the following

$$P_m - P_e = J\omega_m \frac{d\omega_m}{dt} \tag{2}$$

In this equation, J is the moment of inertia of the rotating mass connected to the rotor.

In synchronous generators, in order to control the grid frequency, a speed governor controls the input mechanical power. As a result, the generator output power depends on the input mechanical power and a derivative term that introduces the rotating mass inertia. In a DFIG, where Pm is undispatchable, the output electrical power is controlled directly. Therefore, the grid frequency variation and the rotating mass inertia do not affect the amount of generator output power. Thus, the DFIG inertia does not participate in frequency tuning.

If equation (2) is written in the per unit form, it is as follows:

$$P_m - P_e = 2H\omega_m \frac{d\omega_m}{dt} \tag{3}$$

In this equation, H is the DFIG inertia constant and P_e is equal to $P_{m,\,opt}$. After linearization around the basis rotational speed ω_{m0} (3) can be represented as:

$$\Delta P_m - \Delta P_e = 2Hw_{m0}\frac{d\Delta w_m}{dt} \tag{4}$$

Where,

$$\Delta P_e = 3K_{opt}\omega_{m0}^2\Delta\omega_m \tag{5}$$

To implement virtual inertia, the output electrical power control is changed in such a way that, moreover to tracking the maximum power point, it also responds to system frequency variations. Therefore, the above equation can be modified as follows:

$$\Delta P_e = 3K_{opt}\omega_{m0}^2\Delta\omega_m - H_v(s)\omega_{m0}\Delta\omega \tag{6}$$

In the above equation, the frequency of the grid is represented by ω and $H_v(s)$ is the transfer function of virtual inertia, which represented as follows [22]:

$$H_v(s) = \frac{M_v s}{(\tau_1 s+1)(\tau_2 s+1)} \tag{7}$$

In the above transfer function, M_V is the virtual inertial constant, and τ_1 and τ_2 are the virtual inertia time constants. At low frequencies, $H_v(s)$ behaves similarly to a derivative.

By replacing (6) in (4) we can write:

$$\Delta P_m = 3K_{opt}\omega_{m0}^2\Delta\omega_m - H_V(s)\omega_{m0}\Delta\omega + 2H\omega_{m0}s\Delta\omega_m \tag{8}$$

Using the above equation $\Delta\omega_m$ is obtained according to the equation (9).

$$\Delta\omega_m = \frac{1}{2Hw_{m0}s + 3K_{opt}\omega_{m0}^2}\Delta P_m + \frac{H_V(s)\omega_{m0}}{2Hw_{m0}s + 3K_{opt}\omega_{m0}^2}\Delta\omega \tag{9}$$

By replacing (9) in (6) we will have:

$$\Delta P_e = \frac{3K_{opt}w_{m0}}{2Hs+3K_{opt}w_{m0}}\Delta P_m - \frac{2HH_V(s)\omega_{m0}s}{2Hs+3K_{opt}w_{m0}}\Delta\omega \tag{10}$$

Based on (10), ΔP_e can be changed as a function of ΔP_m and $\Delta\omega$. Therefore, the grid frequency variation and the virtual inertia affect the amount of DFIG output power. By setting M_V and consequently $H_v(s)$ to zero, wind generator without virtual inertia can be represented. The electrical output of DFIG with virtual inertia can be expressed as follows:

$$P_e = P_{m,opt} - M_V \omega_m \frac{d\omega}{dt} \quad (11)$$

Figure 2 shows adding of virtual inertia to the wind turbine equipped with DFIG in the studied islanded MG. In this figure, the transfer functions $G_1(s)$ and $G_2(s)$ are respectively the first and second part of the equation (10).

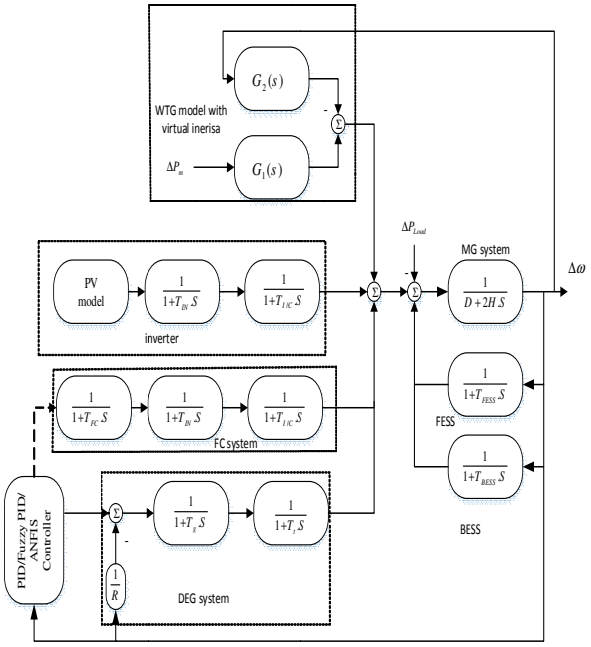


Fig.2. the schematic block diagram of the studied islanded MG with virtual inertia.

IV. FUZZY PID AN ANFIS-BASED CONTROLLER SESIGN

In conventional power systems, conventional PI and PID controllers are often used in the secondary frequency control loop. The operation of these controllers pertains on the values of the proportional, integral and derivative parameters. Using conventional PI and PID controllers, with fix parameters' value, is not guaranteed to achieve the desired performance for different operation conditions and in presence of disturbances and uncertainties. While the PID controller parameters can automatically tune matching to the variations that happen in the grid, the desired performance achievable. One of the features of Fuzzy PID and ANFIS-based controllers is the automatic adjustment of parameters.

The aim of this part is to design a Fuzzy PID and an ANFIS-based controller for complementary control loop in a MG that is separated from the MG. Figure 3 shows the block diagram of the secondary frequency control using the fuzzy PID and ANFIS-based controller. The overall structure of Fuzzy PID Controller is illustrated in Fig. 4.

A. Design of Fuzzy PID Controller

Fuzzy rules have been created based on human knowledge. In this study, the fuzzy block has two inputs, one of which is the MG frequency error, and the other is derived from the MG frequency error. The law that has been written for this block is 49 laws; these rules are fully written in table 3. The range of membership functions for inputs and outputs is between -3 and +3 as shown in Figure 5.

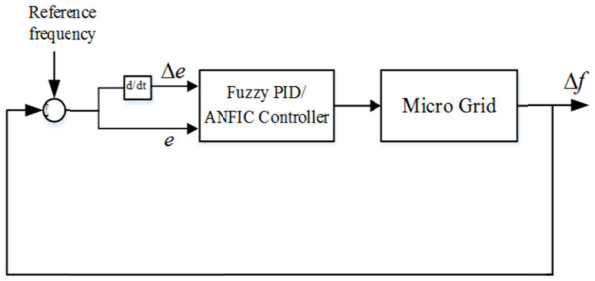


Fig.3. Block diagram of the MG frequency control

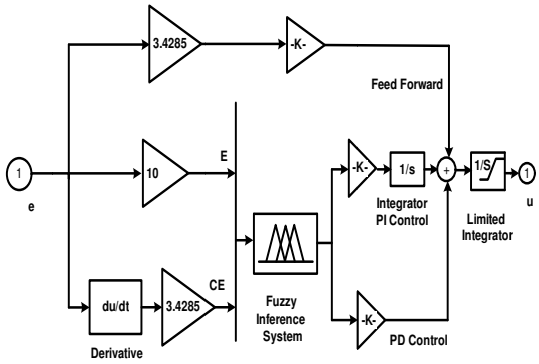
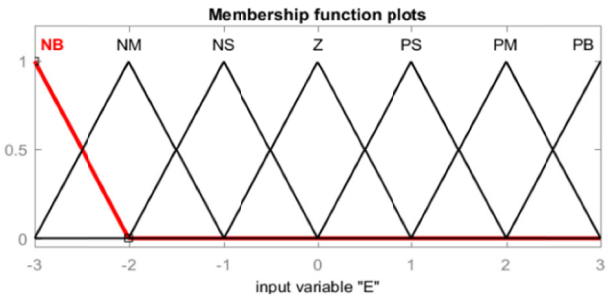


Fig. 4. The overall structure of Fuzzy PID Controller

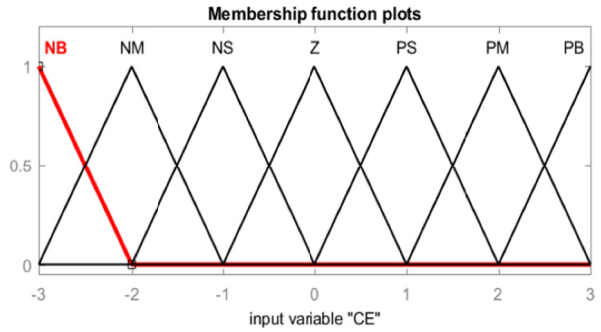
TABLE III . TABLE OF FUZZY RULES

CE / E	NB	NM	NS	Z	PS	PM	PB
NB	NB	NS	NB	NB	NM	NS	Z
NM	NB	Z	NB	NM	NS	Z	PS
NS	NB	PS	NM	NS	Z	PS	PM
Z	NB	PM	NS	Z	PS	PM	PB
PS	NM	PB	Z	PS	PM	PB	PB
PM	NS	Z	PS	PM	PB	PB	PB
PB	Z	PS	PM	PB	PB	PB	PB

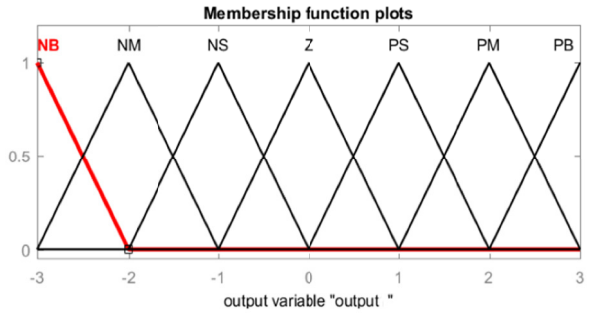


(a)

Fig.5 Continued



(b)



(c)

Fig. 5. Membership functions: a) The error input of the fuzzy block, b) Second input of the fuzzy block (Error derivative) c) output of fuzzy block.

B. Design of ANFIS-based controller

The behaviour of the neuro-fuzzy controller is similar to the fuzzy controller and the only difference between them is that the neural system has been added. To design the proposed ANFIS-based controller, the training data must first be computed. Since the purpose of modelling this controller is to attain the highest control proficiency, for the training of the neural network, first, we apply classical and fuzzy controllers to the studied MG as complementary control. Considering different scenarios such as load variation and parametric uncertainties, the output of each two controllers have been recorded separately. These recorded data are finally have been used to teach the proposed ANFIS-based controller.

The neural network used in this article has five layers. The fuzzy system has 49 rules that the ANFIS system reduced this amounts to two. It is supposed that the fuzzy system has two inputs (x, y), one of which is an error (x = e), and the other is an error derivative (y = de) and has an output z =f (x, y). The rules, if and then the fuzzy, which are in the Takagi and Sugeno type, are the foundation of the fuzzy rules that for a first-order Sugeno system, it produces two rules that are described below.

Rule 1: if x is A_1 and y is B_1 then:

$$f_1 = P_1 e + R_1 \Delta e + s_1 \tag{12}$$

Rule 2: if x is A_2 and y is B_2 then:

$$f_2 = P_2 e + R_2 \Delta e + s_2 \tag{13}$$

Where

$$e = \omega_{ref} - \omega_r \tag{14}$$

$$\Delta e = \frac{d(\omega_{ref} - \omega_r)}{dt} \tag{15}$$

Where, ω_{ref} is the reference angular speed.

The structure of designed ANFIS is depictured in Figure 6. As shown in Fig.6, the output of ANFIS can be represented by,

$$f = \frac{w_1 f_1 + w_2 f_2}{w_1 + w_2} = \overline{w}_1 f_1 + \overline{w}_2 f_2 \tag{16}$$

Weights of the w_1 and w_2 are obtained as the product of the preceding layer outputs and the output f is a weighted average of the two rules outputs [23, 24].

The neural network structure is composed of five layers connected together with the notations $L_{j,i}$ for the output node i from layer j for the five layers.

ANFIS model can be defined as below.

Layer 1: In a layer, the i-th node corresponds to the node function defined by

$$\begin{aligned} L_{1,i} &= \mu_{A_i}(e) \\ L_{1,i} &= \mu_{B_{i-2}}(\Delta e) \end{aligned} \tag{17}$$

Where e and Δe are input to a node and A_i and B_{i-2} are assigned fuzzy function to the node. Layer 1 is consisting of the input variables (membership functions). Membership functions can be defined as triangular form or Gaussian, and so on. For example, A_i can be membership by Gaussian function parameters as follows:

$$\mu_{A_i}(e) = \frac{1}{1 + \left[\left(\frac{e - c_i}{a_i}\right)^2\right]^{b_i}} \tag{18}$$

Layer 2: each node in which layer is a constant node that computes the firing power w_i of a rule. The output of every node is the result of whole the entry signals to it and is defined by,

$$L_{2,i} = W_i = \mu_{A_i}(e)\mu_{B_i}(\Delta e) \tag{19}$$

Layer 3: every node in which layer is a constant node. Each i-th node computes the respect of the i-th rule's firing power

to the aggregate of firing powers of whole the rules. The output from the i-th node is the normalized firing power defined by,

$$L_{3,i} = \overline{W}_i = \frac{W_i}{W_1 + W_2} \qquad i = 1, 2 \qquad (20)$$

Layer 4: In a layer, the i-th node corresponds to the node function defined by,

$$L_{4,i} = \overline{W}_i * f_i = \overline{W}_i.(P_i e + R_i \Delta e + s_i) \qquad i=1,2 \qquad (21)$$

Where $\overline{W}_i$is the output of Layer 3 and $\{P_i, R_i, s_i\}$ is the resultant parameter collection.

Layer 5: This layer contains just one constant node that computes the total output as the aggregate of whole entry signals, i.e.

$$L_{5,i} = \sum_i \overline{W}_i.f_i = \frac{\sum_i W_i f_i}{\sum_i W_i} \qquad (22)$$

The base fuzzy system has 49 rules (Figure 7), which for the ANFIS reduced this value to 2. The structure of the designed ANFIS-based controller in MATLAB illustrated in Figure 8.

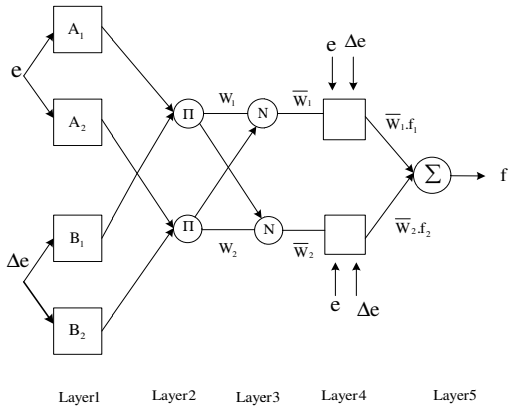


Fig. 6. The structure of the designed ANFIS controller

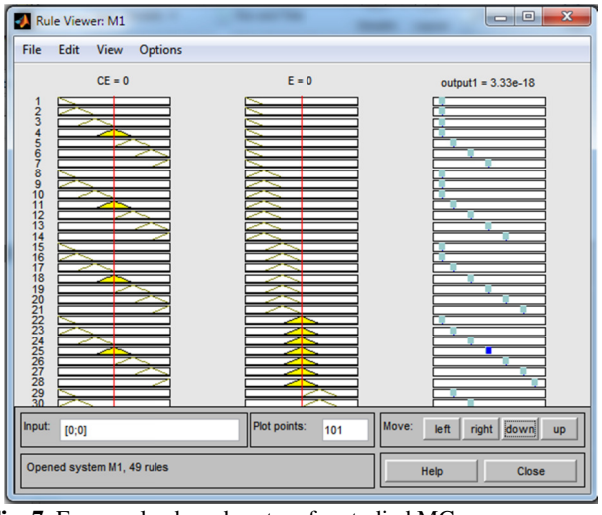


Fig. 7. Fuzzy rules-based system for studied MG

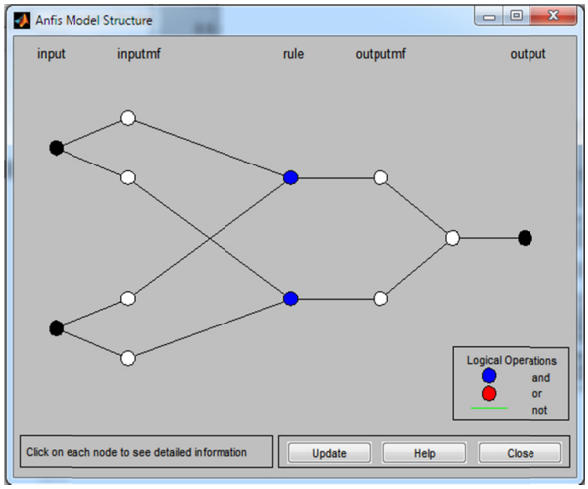


Fig. 8. The Structure of designed ANFIS-based controller in Matlab

V. SIMULATION RESULTS

In this part, the effect of the virtual inertia on the studied MG short-period frequency regulation investigated. In addition, the performance of conventional PID, fuzzy PID and ANFIS-based controllers for frequency regulation considering with and without the virtual inertia is compared. Furthermore, robustness and performance of controllers are investigated in the attendance of different disturbances and uncertainties parametric. In all test scenarios, the conventional PID controller parameters have the same value. Table 4 shows these parameters, which are obtained using the Ziegler-Nichols method.

A. Scenario 1: Step load variation

In this scenario, %10 step load variation (ΔP_L = 0.1 pu) is occurred at t = 1 s. Fig. 9 display the effect of virtual inertia on the short-period frequency regulation when secondary frequency control is performed by a conventional PID. This figure illustrates that implementing virtual inertia improves the MG dynamic response and reduces the short-term frequency variation. Moreover, as one can see in figure 9, increasing M_V leads to less short-period frequency aberration. In addition, the steady-state frequency error is zero regardless of the deal of M_V.

The same step load variation is used to evaluate and compare the performance and efficacy of fuzzy PID and ANFIS-based controllers for frequency regulation. Figure 10 depicts the simulation results considering M_V equal to 10. This figure demonstrates that fuzzy PID and ANFIS-based controllers ameliorate the dynamic response of the LFC compared with classical PID controller. In addition, the settling time, overshoot and undershoot are reduced by using the ANFIS-based controller compared with the fuzzy PID controller.

B. *Scenario 2: Step load variation with parametric uncertainties*

In this case, first, each parameter is varied separately, and then the effect of simultaneously changes in the system parameters and modelling errors are considered as a worst case to evaluate the controllers' robustness. Fig. 11 to Fig. 14 show the effect of parameters change on the frequency regulation when a conventional PID performs the secondary frequency control. Fig. 11 illustrates the MG frequency response considering T_g and T_t variations when M_V is equal to 3. As one can see the augmentation of the governor and turbine time constant degrade the MG dynamic response. The effect of 50% variation in H and D are presented in Fig. 12 and 13 for M_V equal to 3 and 0.5, respectively. These figures show that the reduction of load sensitivity coefficient degrades noticeably the MG dynamic response when M_V is equal to 0.5. In addition, due to the small amount of the parameter H, its variations have little effect on the MG frequency's behavior. Figure 14 depicts the effect of 50% variation in R, T_{FESS} and T_{BESS} on the frequency regulation. This figure shows that the reduction of R decreases the MG stability and increasing of R leads to more frequency deviation. Furthermore, due to the small amount of the parameters T_{FESS} and T_{BESS}, their variations have little effect on the frequency regulation.

Table 5 shows the intended system parameters variations and modelling errors as a worst case. The simulation results are presented in Fig. 15 and Fig. 16 for this case. As Fig. 15 shown the studied MG become unstable when the controller is conventional PID. Zoomed results are illustrated in Fig. 16. As one can see, in this case, with the Fuzzy-PID controller the studied MG has poor stability. Instead, the proposed control strategy (ANFIS-based controller with implemented virtual inertia) regulates properly the MG frequency and its performance is not much affected by the parameters changes.

TABLE IV. PID CONTROLLER PARAMETERS

K_D	K_I	K_P
0.2	*15.19*	*2.3*

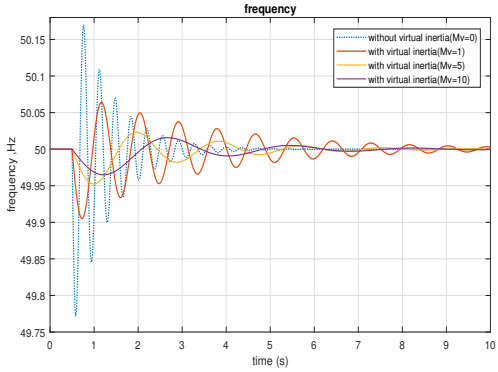


Fig. 9. Impact of virtual inertia on the short-period frequency regulation.

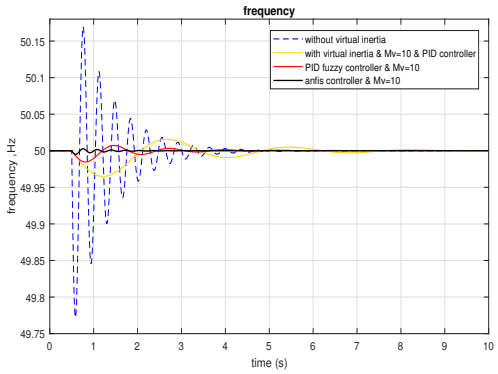


Fig. 10. Performance of different controllers on the short-period frequency adjustment in the attendance of virtual inertia.

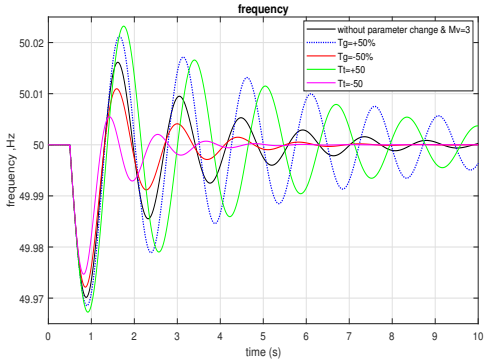


Fig. 11. MG frequency response considering T_g and T_t variations.

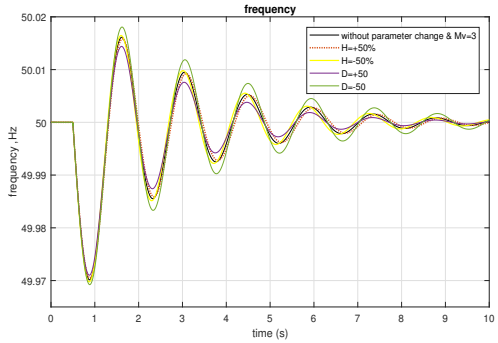


Fig. 12. MG frequency response considering H and D variations for $M_v = 3$

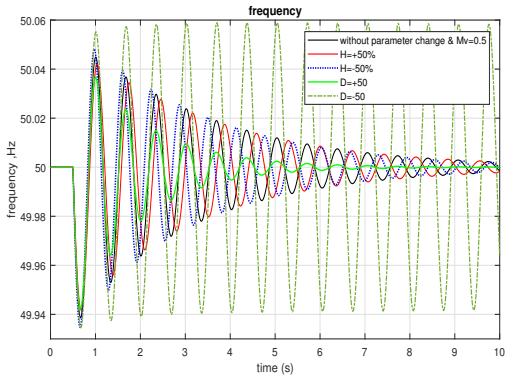


Fig. 13. MG frequency response considering H and D variations for $M_v = 0.5$

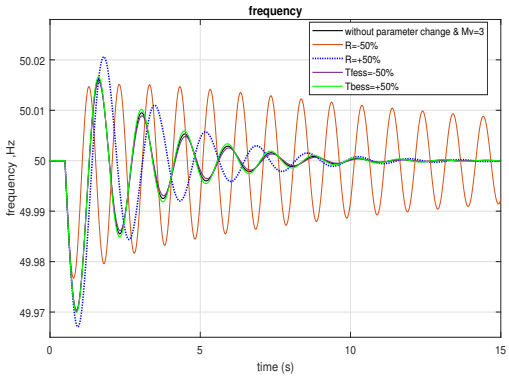


Fig. 14. MG frequency response considering R, TFESS and TBESS variations for$M_v = 3$.

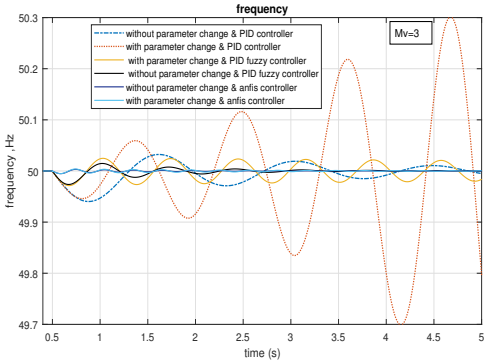


Fig. 15. MG frequency response considering the system parameters variations and modelling errors shown in table 5.

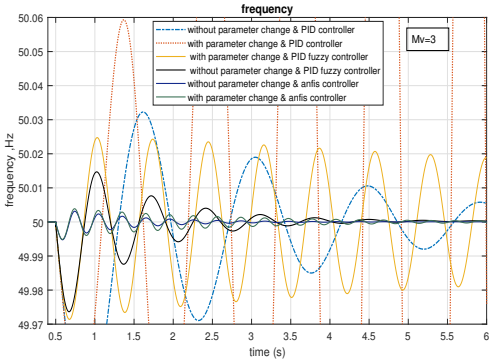


Fig. 16. Zoomed MG frequency response.

C. Scenario 3: Step load variation with parametric uncertainties without energy storage equipment

In this scenario, the conditions are the same as those in the previous scenario. Nevertheless, in this scenario; energy storage equipment has been removed from the system under study. As can be seen in Figure 17 removing energy storage equipment leads to performance degradation of the conventional PID and Fuzzy PID controllers, where both controllers become unstable. However, using the suggested control scheme, the system frequency is effectively regulated even without energy storage equipment. Furthermore, Fig. 18, which compares the effectiveness of Fuzzy PID and ANFIS-based controllers in this scenario, depicts that the system frequency response remains approximately unchanged with and without energy storage equipment. Fig. 19 illustrates the performance of the ANFIS-based controller versus M_v under such conditions. This figure shows that the performance of the ANFIS-based controller is acceptable even with small $M_v = 2$, but $M_v = 1$ leads to MG frequency instability.

VI. CONCLUSION

In this paper, to regulate the frequency of studied islanded MG a control scheme is proposed. The proposed control strategy consists of an ANFIS-based controller as secondary frequency control and a rotating-mass-based virtual inertia, implemented in DFIG control system, as an inherent energy storage system. The simulation conclusions demonstrate that using the suggested control strategy the frequency of studied MG can effectively regulate despite removing energy storage equipment, severe system parameters changes and modelling error. three different controllers are implemented in order to achieve good frequency regulation/tracking regardless of the presence of disturbances and parameter variations. In practice, simple PI&PID controllers are commonly used that provide a poor performance in the presence of serious disturbances and The fuzzy controller is heavily dependent on membership functions. eventually the results reveal that the ANFIS-based controller outperforms other controllers in all aspects such as overshoot, undershoot, steady state error, rise time and settling time.

TABLE V. SYSTEM PARAMETERS CHANGES AND MODELLING ERRORS

Parameter	Value	Parameter	Value
D	-50%	$T_g(s)$	+50%
H(s)	-50%	$T_t(s)$	+50%
$T_{Fess}(s)$	+50%	$T_{Bess}(s)$	+50%
R	-50%		

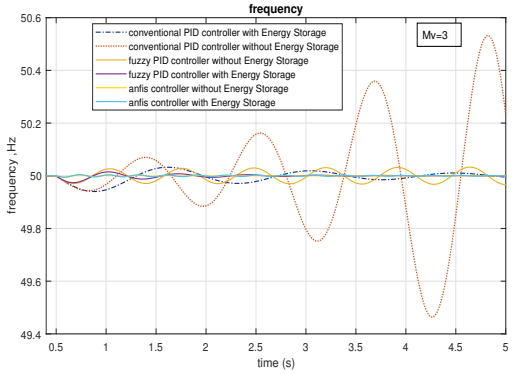


Fig. 17. MG frequency response without energy storage equipment and considering the parameters changes.

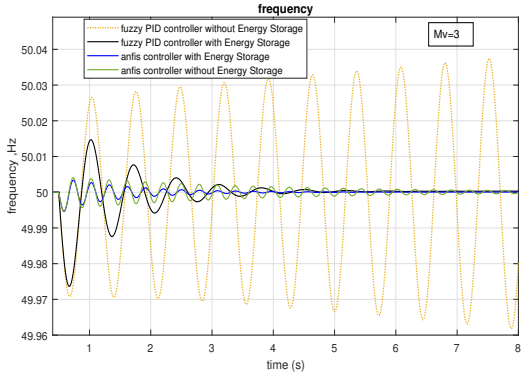


Fig. 18. Zoomed MG frequency response without energy storage equipment and considering the parameters changes.

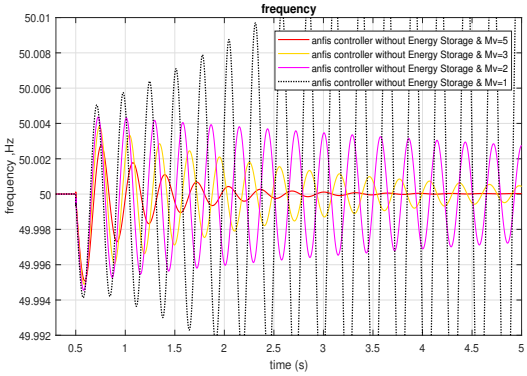


Fig. 19. Performance of ANFIS-based controller versus M_v without energy storage equipment and considering the parameters changes.

REFERENCES

[1] Y. Fu, Y. Wang, and X. Zhang.: 'integrated wind turbine controller with virtual inertia and primary frequency responses for grid dynamic frequency support' IET Renewable Power Generation., 2017, 11, (8), pp. 1129 – 1137.

[2] M. Heidari., 'Maximum Wind Energy Extraction by Using Neural Network Estimation and Predictive Control of Boost Converter' International Journal of Industrial Electronics, Control and Optimization. Vol. 1, No. 2, pp. 115-120, September (2018).

[3] D. Wang et al., "Participation in primary frequency regulation of wind turbines using hybrid control method", International Transactions on Electrical Energy Systems, 2018, 28, (5).

[4] M. Fazeli, G. M. Asher, C.Klumpner, and L.Yao, 'Novel integration of DFIG-based wind generators within microgrids' IEEE Trans. Energy Convers., 2011, 26, pp. 840–850.

[5] G. Ramtharan, N. Jenkins, J.B. Ekanayake.: 'Frequency support from doubly fed induction generator wind turbines". IET Renewable Power Generation'., 2007, 1, (1), pp. 3-9.

[6] N. John and K. Ramesh.: 'Enhancement of load frequency control concerning high penetration of wind turbine using PSO-fuzzy technique', International Journal of Computer Applications., 2013, 69, No 14.

[7] Y. Fu, Y. Wang, X. Zhang.: 'An Integrated Wind Turbine Controller with Virtual Inertia and Primary Frequency Responses for Grid Dynamic Frequency Support', IET Renewable Power Generation., 2017, 11, (8), pp.1129 – 1137.

[8] P.Li, W.Hu, R.Hu, Z.Chen.: 'The Integrated Control Strategy for Primary Frequency Control of DFIGs Based on Virtual Inertia and Pitch Control', Innovative Smart Grid Technologies - Asia, Dec 2016, pp.430 - 435.

[9] Q.-C. Zhong and G.Weiss.: 'Synchronverters: Inverters that mimic synchronous generators', IEEE Transactions on Industrial Electronics., 2011, 58, no. 4, pp. 1259–1267.

[10] M. Torres and L. A. C. Lopes.: 'Virtual synchronous generator control in autonomous wind-diesel power systems', in Proc. IEEE Electrical Power & Energy Conf. (EPEC), 2009, pp. 1–6.

[11] G. Delille, B. Francois, G. Malarange.: 'Dynamic frequency control support: A virtual inertia provided by distributed energy storage to isolated power systems', presented at the IEEE Power and Energy Soc. Innovative Smart Grid Technol. Europe, Oct 2010, pp. 11–13.

[12] D. Gautam, L. Goel, R. Ayyanar, V. Vittal, and T. Harbour.: 'Control strategy to mitigate the impact of reduced inertia due to doubly fed induction generators on large power systems', IEEE Transactions on Power Systems., 2011, vol. 26, pp. 214–224.

[13] L.-R. Chang-Chien, W.-T.Lin and Y.-C. Yin.: 'Enhancing frequency response control by DFIGs in the high wind penetrated power systems', IEEE Transactions on Power Systems., 2011, 26, pp. 710–718.

[14] Xiaorong. Zhu, Yi Wang, Lie Xu, Xiangyu Zhang, and Heming Li.: 'Virtual inertia control of DFIG based wind turbines for dynamic grid frequency support', IET Conf. Renewable Power Generation, Edinburgh., 2011, pp.16.

[15] L. Zeni, I. D. Margaris, A. D. Hansen, P. Sørensen.: 'Virtual inertia for variable speed wind turbines', Wind Energy., 2012, 16, (8), pp. 1225-1239.

[16] Z. Q. Wu and Mizumoto.: 'PID type fuzzy controller and parameter adaptive method', Fuzzy Sets and System., 1996, 78, (1), pp.23-36.

[17] H. Ameli et al., "A fuzzy-logic–based control methodology for secure operation of a microgrid in interconnected and isolated modes", International Transactions on Electrical Energy Systems, 2017, 27,(11).

[18] S. A. Taher, R. Hematti, A. Abdolalipour, and S. H. Tabei.: 'Optimal decentralized load frequency control using HPSO algorithms in deregulated power systems', American

Journal of Applied Sciences, 2008, 5, pp. 1167-1174.
[19] H. Bevrani and P. R. Daneshmand.: 'Fuzzy logic-based load-frequency control concerning high penetration of wind turbines', IEEE Syst. J., 2012, 6, pp. 173–180.
[20] Bevrani H, Habibi F, Babahajyani P, Watanabe M, Mitani Y.: 'On-line PSO-based fuzzy tuning approach'. IEEE Transaction on Smart Grids, 2012, 3, (99), pp. 1935-1944.
[21] K.V. Shihabudheen et al., 'Control for grid-connected DFIG-based wind energy system using adaptive neuro-fuzzy technique', International Transactions on Electrical Energy Systems, 2018, 28, (5).
[22] M. F.-M. Arani and E. F. El-Saadany, 'Implementing virtual inertia in DFIG-based wind power generation' ,IEEE Transactions on Power Systems, 2013, 28, (2), pp. 1373-1384, 2013.
[23] J.S.R. Jang.: 'ANFIS: Adaptive network- based fuzzy inference system', IEEE Trans. Sys. Man. Cyb., 1993, 23, (3), pp.665-685.
[24] A. Chikh, A. Chandra.: 'Adaptive neuro-fuzzy based solar cell model', IET Renewable Power Generation., 2014, 8, (6), pp. 679-686.



Akbar karimipouya was born in Andimeshk, Khuzestan, Iran. He received the B.Sc. degree from Jundishapur University of Technology, Iran, in 2011, M.Sc. degree in electrical power systems from the Kurdistan University, Iran in 2013. He is currently pursuing his Ph.D. in electrical engineering at Razi University, Kermanshah, Iran. He's main research interest is Micro grid frequency control, drives and Intelligent controllers. He works in Khuzestan Water and Power Authority (KWPA).



Shahram Karimi was born in Kermanshah, Iran, in 1972. He received the B.S. degree from University of Tabriz, Tabriz, Iran, in 1995, the M.S. degree from Sharif University of Technology, Tehran, Iran, in 1997, and the Ph.D. degree all in electrical engineering from the Université Henri Poincaré, Nancy, France, in 2008. He is currently an Assistant Professor in Department of Electrical Engineering, Razi University, Kermanshah, Iran. His research interests include Microgrid voltage and frequency control, active power filters, power quality, FACTS Devices and fault tolerant converters.



Hamdi Abdi was born in Paveh, Iran, in July 1973. He received his B.Sc. degree from Tabriz University, Tabriz, Iran in 1995; M.Sc., and Ph.D. degrees from Tarbiat Modares University, Tehran, Iran, in 1999, and 2006, respectively, all in Electrical Engineering. Currently, he is an associate professor in the Department of Electrical Engineering, Razi University, Kermanshah, Iran. His research interests include power system optimization, operation and planning, smart grids, demand response, multi carrier energy system, energy hub, load forecasting, and design of electrical and control systems for industrial plant.